Structure Assignment in the Solid State by the Coupling of Quantum Chemical Calculations with NMR Experiments: A Columnar Hexabenzocoronene Derivative

Christian Ochsenfeld,[†] Steven P. Brown,[‡] Ingo Schnell,[‡] Jürgen Gauss,[†] and Hans Wolfgang Spiess[‡]

Contribution from the Institut für Physikalische Chemie, Universität Mainz, D-55099 Mainz, Germany, and Max-Planck-Institut für Polymerforschung, Postfach 3148, D-55021 Mainz, Germany

Received June 19, 2000. Revised Manuscript Received December 13, 2000

Abstract: We present a quantum chemical ab initio study which demonstrates a new combined experimental and theoretical approach, whereby a comparison of calculated and experimental ^{1}H NMR chemical shifts allows the elucidation of structural arrangements in solid-state molecular ensembles, taking advantage of the marked sensitivity of the ^{1}H chemical shift to intermolecular interactions. Recently, Brown et al. have shown that, under fast magic-angle spinning (MAS) at 35 kHz, the resolution in a ^{1}H NMR spectrum of the solid phase of an alkyl-substituted hexabenzocoronene (HBC) derivative is sufficient to observe the hitherto unexpected resolution of three distinct aromatic resonances (*J. Am. Chem. Soc.* **1999**, *121*, 6712). Exploiting the additional information about proton proximities provided by ^{1}H double-quantum (DQ) MAS NMR spectroscopy, it was shown that the results are qualitatively consistent with the aromatic cores packing in a manner similar to that in unsubstituted HBC. Using the HBC-C_{12} molecule as an example, we show here that the new combined experimental and theoretical approach allows the observed ^{1}H chemical shifts to be related in a *quantitative* manner to the intermolecular structure. In the quantum chemical calculations, a series of model systems of stacked HBC oligomers are used. On account of the marked dependence of the ^{1}H chemical shift to ring currents arising from nearby aromatic rings, the calculated ^{1}H chemical shifts are found to be very sensitive to the stacking arrangement of the HBC molecules. Moreover, the ring current effect is found to be particularly long range, with a considerable influence of the second neighbor, at a distance of 700 pm, being observed.

Introduction

Over the past two decades, quantum chemistry has developed into a powerful tool for studying the structures and properties of molecular systems. In many chemical investigations, ab initio calculations are now used to supplement and facilitate the interpretation of experiments, to perform systematic studies where experiments are not feasible, or even to suggest new experiments (see refs 1 and 2 for overviews and examples). Though quantum chemical calculations were originally restricted to rather small molecular systems, important methodological developments (e.g., refs 3−7) coupled with the steep increase in computing power means that today the handling of molecules of the order of 100 atoms at the Hartree−Fock (HF) and density functional theory (DFT) level is routinely possible. More recent developments extend these limits even further to much larger molecular systems of more than 500−1000 atoms (e.g., refs 8−14), such that the contribution of quantum chemical calculations to the understanding of chemical systems is becoming ever more important.

An especially useful link to experiment is provided by the quantum chemical calculation of NMR chemical shifts;[15−18] such calculations have facilitated, in numerous cases, the unequivocal assignment of experimental spectra, in particular in the areas of carbocation and borane chemistry.[15] Quantum chemical calculations have not only been combined with solution-state NMR studies but also with solid-state MAS NMR experiments (e.g., refs 19 and 20). The routine calculation of NMR chemical shifts[21−23] has only become possible because of the introduction

[†] Universität Mainz.
[‡] Max-Planck-Institut für Polymerforschung.

(1) Ahlrichs, R.; Elliott, S. D.; Huniar, U. *Ber. Bunsen-Ges. Phys. Chem.* **1998**, *102*, 795.
(2) Head-Gordon, M. *J. Phys. Chem.* **1996**, *100*, 13213.
(3) Almlöf, J.; Faegri, K., Jr.; Korsell, K. *J. Comput. Chem.* **1982**, *3*, 385.
(4) Cremer, D.; Gauss, J. *J. Comput. Chem.* **1986**, *7*, 274.
(5) Häser, M.; Ahlrichs, R. *J. Comput. Chem.* **1989**, *10*, 104.
(6) Pulay, P. *Mol. Phys.* **1969**, *17*, 197.
(7) Pulay, P. *Adv. Chem. Phys.* **1987**, *69*, 241.
(8) White, C. A.; Head-Gordon, M. *Chem. Phys. Lett.* **1994**, *230*, 8.
(9) Challacombe, M.; Schwegler, E.; Almlöf, J. *J. Chem. Phys.* **1996**, *104*, 4685.
(10) Ochsenfeld, C.; Head-Gordon, M. *Chem. Phys. Lett.* **1997**, *270*, 399.
(11) Ochsenfeld, C.; White, C. A.; Head-Gordon, M. *J. Chem. Phys.* **1998**, *109*, 1663.
(12) Scuseria, G. E. *J. Phys. Chem.* **1999**, *A 103*, 4782.
(13) Ochsenfeld, C. *Chem. Phys. Lett.* **2000**, *327*, 216.
(14) Eichkorn, K.; Treutler, O.; Öhm, H.; Häser, M.; Ahlrichs, R. *Chem. Phys. Lett.* **1995**, *240*, 283.
(15) Bühl, M. Structural Applications of NMR Chemical Shift Computations. In *Encyclopedia of Computational Chemistry*; Schleyer, P. v. R., Allinger, N. L., Clark, T., Gasteiger, J., Kollman, P. A., Schaefer, H. F., III, Schreiner, P. R., Eds.; Wiley: Chichester, 1998; pp 1835−1845.
(16) Pulay, P.; Hinton, J. F. In *Encyclopedia of Nuclear Magnetic Resonance*; Grant, D. M., Harris, R. K., Eds.; Wiley: Chichester, 1996; Vol. 7, p 4334.
(17) Facelli, J. C. In *Encyclopedia of Nuclear Magnetic Resonance*; Grant, D. M., Harris, R. K., Eds.; Wiley: Chichester, 1996; Vol. 7, p 4327.
(18) de Dios, A. C. *Prog. NMR Spectrosc.* **1996**, *29*, 229.
(19) Facelli, J. C.; Grant, D. M. *Nature* **1993**, *365*, 325.
(20) Salzmann, R.; Ziegler, C. J.; Godbout, N.; McMahon, M. T.; Suslick, K. S.; Oldfield, E. *J. Am. Chem. Soc.* **1998**, *120*, 11323.
(21) Gauss, J. *Ber. Bunsen-Ges. Phys. Chem.* **1995**, *99*, 1001.
(22) Helgaker, T.; Jaszunski, M.; Ruud, K. *Chem. Rev.* **1999**, *99*, 293.

10.1021/ja0021823 CCC: $20.00
Published on Web 02/27/2001

of so-called local gauge-origin methods,[24−28] which provide a solution to the gauge-origin problem inherent to the approximations associated with quantum chemical calculations.

To date, NMR chemical shift calculations have mainly been applied in cases where comparison with experimental spectra allows the identification of specific molecular connectivities or conformations.[15−18,29,30] Here, we show that by taking advantage of recent advances in solid-state NMR spectroscopy, the scope of the combined experimental and theoretical approach can be extended to provide information about intermolecular interactions and therefore enable the elucidation of structural arrangements in molecular ensembles.

In the solid state the molecular tumbling, which, in the solution state, leads to the observation of inherently high-resolution NMR spectra, is usually absent. Thus, the application of ^{1}H NMR spectroscopy to rigid solids is complicated by strong proton−proton dipolar couplings, which cause a substantial homogeneous broadening of the resonances. Recently, magic-angle spinning (MAS) probes capable of supporting a rotation frequency in excess of 30 kHz have become available. At such a fast rotation frequency, the residual dipolar broadening is reduced to a sufficient extent that resonances due to chemically distinct sites can be resolved.[31−36] Moreover, the combination of fast MAS with two-dimensional double-quantum (DQ) spectroscopy[37,38] allows the determination of valuable structural and dynamical information inherent to the proton−proton dipolar couplings and also leads to a better separation of the ^{1}H resonances because of the extension to a second dimension. On account of the high sensitivity of ^{1}H NMR as well as the presence of protons in a very wide range of systems, these advances are of major importance. In particular, it should be remembered that NMR directly probes the local structure and is thus applicable to samples lacking long-range order, e.g., amorphous polymers,[39] liquid-crystalline phases,[40] and glasses.[41] Furthermore, it should be noted that heteronuclear ^{1}H−^{13}C correlation experiments applicable to naturally abundant samples have recently been developed.[42−44] Due to the much better resolution in the ^{13}C dimension, such experiments allow the ^{1}H chemical shifts of protons bonded to specific carbon atoms to be identified. Employing homonuclear ^{1}H decoupling methods, such as the frequency-switched Lee-Goldburg approach,[45,46] ^{1}H line widths (full width at half-maximum height) of under 500 Hz can be achieved in these experiments. Although even this resolution is still somewhat limited, this is a rapidly changing field, as evidenced by the substantial advances in the past 5 years, and further considerable improvement is to be expected.

It is well-known that the ^{1}H chemical shift is a sensitive probe of hydrogen-bonding and aromatic ring current effects. Taking advantage of the currently achievable ^{1}H solid-state NMR resolution provided by very-fast MAS, we have demonstrated that such ^{1}H chemical shift information can be extracted, thus providing valuable insight into these important intermolecular interactions.[31−35] However, to date, it was only possible to draw qualitative statements from the observed ^{1}H chemical shifts, and as a consequence, the full information content has not been exploited. The challenge therefore remains to relate the observed ^{1}H chemical shifts in a quantitative manner to both the intra- and intermolecular structure and order. In the following, we will demonstrate how this challenge can be tackled by means of quantum chemical calculations and how a reliable structure determination for the solid state can be achieved by an interplay of theory and experiment.

Our example is a hexabenzocoronene (HBC, $C_{42}H_{18}$) derivative synthesized by Müllen and co-workers,[32,47,48] namely, hexa-*n*-dodecylhexa-*peri*-hexabenzocoronene (henceforth referred to as HBC-C_{12}; substituents R = *n*-$C_{12}H_{25}$). In ref 32, Brown et al. have shown that three aromatic resonances can be resolved in the ^{1}H MAS NMR spectrum of HBC-C_{12} (see Figure 1a): 8.3, 6.9, and 5.7 ppm. This observation is surprising since the symmetry of the isolated molecule would predict equivalence of all aromatic protons. Further insight is provided by the aromatic region of a two-dimensional ^{1}H DQ MAS spectrum of HBC-C_{12} as shown in Figure 1b. In such a spectrum, a peak is only observed if the two protons have a close proximity; for HBC-C_{12}, the arrangement of the aromatic protons into well-

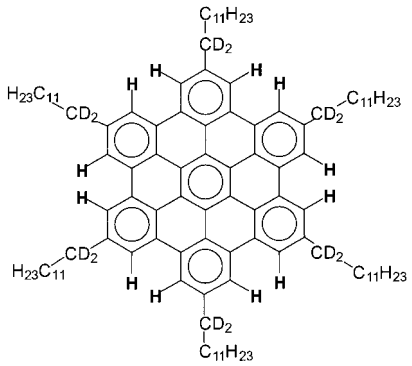

(23) Fleischer, U.; Kutzelnigg, W.; van Wüllen, C. Ab initio NMR Chemical Shift Computation. In *Encyclopedia of Computational Chemistry*; Schleyer, P. v. R., Allinger, N. L., Clark, T., Gasteiger, J., Kollman, P. A., Schaefer, H. F., III, Schreiner, P. R., Eds.; Wiley: Chichester, 1998; pp 1827−1835.
(24) Kutzelnigg, W. *Isr. J. Chem.* **1980**, *19*, 193.
(25) Schindler, M.; Kutzelnigg, W. *J. Chem. Phys.* **1982**, *76*, 1919.
(26) Hansen, A. E.; Bouman, T. D. *J. Chem. Phys.* **1985**, *82*, 5035.
(27) Ditchfield, R. *Mol. Phys.* **1974**, *27*, 789.
(28) Wolinski, K.; Hinton, J. F.; Pulay, P. *J. Am. Chem. Soc.* **1990**, *112*, 8251.
(29) Born, R.; Spiess, H. W. *Macromolecules* **1995**, *28*, 7785.
(30) Born, R.; Spiess, H. W. *NMR basic principles and progress* **1997**, *35*, 1.
(31) Schnell, I.; Brown, S. P.; Low, H. Y.; Ishida, H.; Spiess, H. W. *J. Am. Chem. Soc.* **1998**, *120*, 11784.
(32) Brown, S. P.; Schnell, I.; Brand, J. D.; Müllen, K.; Spiess, H. W. *J. Am. Chem. Soc.* **1999**, *121*, 6712.
(33) Brown, S. P.; Schnell, I.; Brand, J. D.; Müllen, K.; Spiess, H. W. *J. Mol Struct.* **2000**, *521*, 179.
(34) Brown, S. P.; Schnell, I.; Brand, J. D.; Müllen, K.; Spiess, H. W. *Phys. Chem. Chem. Phys.* **2000**, *2*, 1735.
(35) Brown, S. P.; Schaller, T.; Seelbach, U.; Koziol, F.; Ochsenfeld, C.; Klärner, F.-G.; Spiess, H. W. *Angew. Chem. Int. Ed.* **2001**, *40*, 717.
(36) Rodriguez, L. N. J.; De Paul, S. M.; Barrett, C. J.; Reven, L.; Spiess, H. W. *Adv. Mater.* **2000**, *12*, 1934.
(37) Geen, H.; Titman, J. J.; Gottwald, J.; Spiess, H. W. *Chem. Phys. Lett.* **1994**, *227*, 79.
(38) Gottwald, J.; Demco, D. E.; Graf, R.; Spiess, H. W. *J. Magn. Reson.* **1995**, *243*, 314.
(39) Schmidt-Rohr, K.; Spiess, H. W. *Multidimensional Solid State NMR and Polymers*; Academic Press: New York, 1994.
(40) Demus, D., Goodby, J. W., Gray, G. W., Spiess, H. W., Vill, V., Eds. *Handbook of Liquid Crystals*; Wiley-VCH: Weinheim, 1998.
(41) Eckert, H. *NMR basic principles and progress*; **1994**, *33*, 125.
(42) van Rossum, B.-J.; Förster, H.; De Groot, H. J. M. *J. Magn. Reson.* **1996**, *124*, 516.
(43) Lesage, A.; Sakellariou, D.; Steuernagel, S.; Emsley, L. *J. Am. Chem. Soc.* **1998**, *120*, 13194.
(44) Saalwächter, K.; Graf, R.; Spiess, H. W. *J. Magn. Reson.* **1999**, *140*, 471.
(45) Bielecki, A.; Kolbert, A. C.; Levitt, M. H. *Chem. Phys. Lett.* **1989**, *155*, 341.
(46) Levitt, M. H.; Kolbert, A. C.; Bielecki, A.; Ruben, D. J. *Solid State NMR* **1993**, *2*, 151.
(47) Herwig, P.; Kayser, C. W.; Müllen, K.; Spiess, H. W. *Adv. Mater.* **1996**, *8*, 510.
(48) Van de Craats, A. M.; Warman, J. M.; Fechtenkötter, A.; Brand, J. D.; Harbison, M. A.; Müllen, K. *Adv. Mater.* **1999**, *11*, 1469.

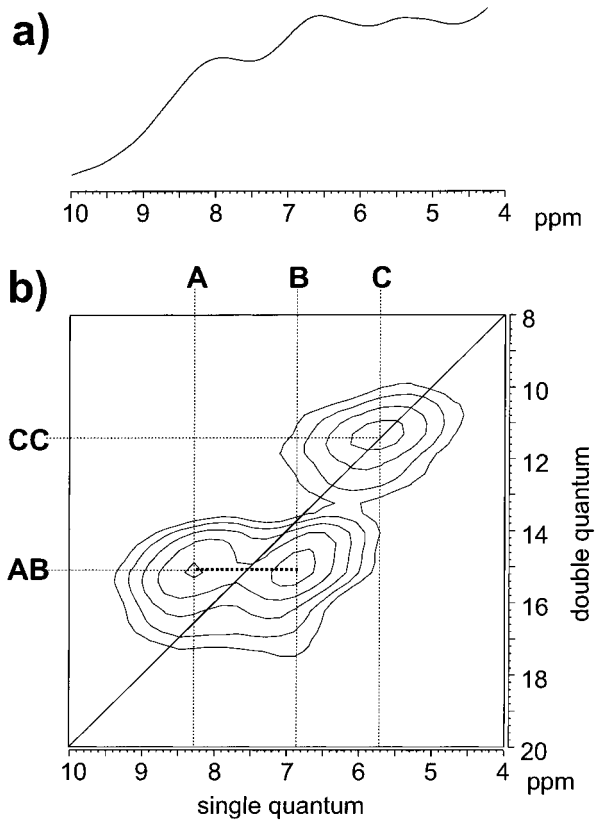

Figure 1. Experimental ^{1}H (500.1 MHz) NMR spectra of an HBC-C_{12} sample, in which the alkyl side chains are deuterated at the α position to 87%. The aromatic regions of the (a) MAS and (b) DQ MAS spectra are shown. The MAS frequency was 35 kHz. Further experimental details are given in ref 32.

isolated "bay" proton pairs means that the observed DQ peaks can only arise from such pairs. Of the six possible DQ peaks, only AB cross-peaks and a CC diagonal peak are observed. This implies the existence of only two different types of bay proton pairs: one (AB) where two neighboring aromatic protons have different chemical shifts, namely, 8.3 and 6.9 ppm, and the other (CC) where the two protons both have the same chemical shift of 5.7 ppm. It should be noted that the spectra in Figure 1 were obtained for a sample where the α-carbons of the alkyl side chains were deuterated (87%). This has the effect of reducing the line widths of the aromatic resonances, due to the reduced number of dipolar-coupled protons. However, as demonstrated in ref 32, exactly the same experimental features were observed for a fully protonated sample, albeit with somewhat poorer resolution.

On the basis of an X-ray investigation of the unsubstituted HBC system[49]—it was not possible to prepare a single crystal suitable for an X-ray diffraction study for HBC-C_{12}—a columnar arrangement of the HBC molecules appears plausible, where the different layers, each consisting of one HBC molecule, are shifted with respect to each other. In this packing arrangement, strong magnetic anisotropies (ring currents) associated with aromatic systems (see refs 50−52) are expected to have an important influence on the ^{1}H chemical shifts. Making this assumption, Brown et al.[32] have proposed a specific solid-state structure model for HBC-C_{12} on the basis of the measured ^{1}H chemical shifts, the proximity information from the ^{1}H DQ NMR spectrum, and a simple empirical ring current model. However, a confirmation of the suggested structure on the basis of more rigorous quantum chemical calculations is still lacking. This gives us the opportunity to demonstrate the combined use of experiment and quantum chemical calculations to elucidate solid-state structures. Therefore, in this paper, we will put the proposed structure model for the HBC derivative HBC-C_{12} on a more rigorous basis, and in this way outline a general, and in our opinion very promising, scheme for future solid-state structure determinations.

Theoretical Approach

Model Structures. The presence of the long alkyl chains in the HBC-C_{12} system prevents the close approach of the HBC cores in all but one dimension. The strong separation of the columns in HBC-C_{12} then suggests that it is sufficient to restrict the quantum chemical calculations to the study of a single HBC column. Since NMR chemical shifts are considered to be "local" properties, it seems reasonable to further simplify the system to be computed by using fragments, i.e., oligomers, of the solid-state column. In addition, the influence of the alkyl chains on the chemical shifts is estimated in selected smaller model systems, thus allowing the use of unsubstituted HBC oligomers to model the solid-state structure. These simplifications are important for the feasibility of quantum chemical calculations on these large molecular systems within a reasonable time frame. It is, however, crucial to monitor the reliability of the chosen model system and to pay special attention to the convergence of molecular properties with oligomer size and with it the dependence of ^{1}H chemical shifts on the separation of the monomer layers.

Computational Details. Ab initio calculations were performed using the program packages Q-Chem[53] and TURBOMOLE.[54] Geometry optimizations were carried out at HF, MP2 (second-order Møller−Plesset perturbation theory),[55] and DFT (using the BP86 functional)[56−58] levels. The computationally more demanding MP2 method explicitly includes electron correlation effects missing in the HF approach. For the molecules considered in this study, a comparison with the MP2 results allows the accuracy of the HF and DFT methods to be assessed.

To avoid the gauge-origin problem in the calculation of NMR chemical shifts, we use the gauge including atomic orbitals (GIAO)[27,28,59] approach, which has been particularly successful for the calculation of chemical shifts.[21] The accuracy of the GIAO scheme at the HF level (GIAO-HF)[27,28,60] for the present molecular systems was checked by GIAO-MP2 calculations[61−63]

(49) Goddard, R.; Haenel, M. W.; Herndon, W. C.; Krüger, C.; Zander, M. *J. Am. Chem. Soc.* **1995**, *117*, 30.
(50) Schleyer, P. v. R.; Jiao, H. J. *Pure Appl. Chem.* **1996**, *68*, 209.
(51) Juselius, J.; Sundholm, D. *Phys. Chem. Chem. Phys.* **1999**, *1*, 3429.
(52) Lazzeretti, P. *Prog. NMR Spectrosc.* **2000**, *36*, 1.
(53) White, C. A.; Kong, J.; Maurice, D. R.; Adams, T. R.; Baker, J.; Challacombe, M.; Schwegler, E.; Dombroski, J. P.; Ochsenfeld, C.; Oumi, M.; Furlani, T. R.; Florian, J.; Adamson, R. D.; Nair, N.; Lee, A. M.; Ishikawa, N.; Graham, R. L.; Warshel, A.; Johnson, B. G.; Gill, P. M. W.; Head-Gordon, M. *Q-Chem*; Q-Chem Inc.: Pittsburgh, PA, 1998, development version.
(54) Ahlrichs, R.; Bär, M.; Häser, M.; Horn, H.; Kölmel, C. *Chem. Phys. Lett.* **1989**, *162*, 165.
(55) Møller, C.; Plesset, M. S. *Phys. Rev.* **1934**, *46*, 618.
(56) Parr, R. G.; Yang, W. *Density-Functional Theory of Atoms and Molecules*; Oxford University Press: New York, 1989, and references therein.
(57) Perdew, J. P. *Phys. Rev. B* **1986**, *33*, 8822.
(58) Becke, A. D. *Phys. Rev. B* **1988**, *38*, 3098.
(59) London, F. *J. Phys. Radium* **1937**, *8*, 397.
(60) Häser, M.; Ahlrichs, R.; Baron, H. P.; Weis, P.; Horn, H. *Theor. Chim. Acta* **1992**, *83*, 455.
(61) Gauss, J. *Chem. Phys. Lett.* **1992**, *191*, 614.
(62) Kollwitz, M.; Gauss, J. *Chem. Phys. Lett.* **1996**, *260*, 639.
(63) Kollwitz, M.; Häser, M.; Gauss, J. *J. Chem. Phys.* **1998**, *108*, 8295.

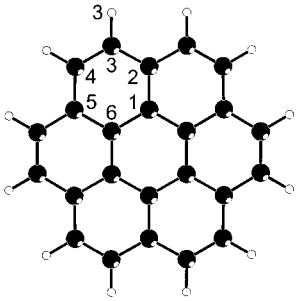

Figure 2. The structure of coronene, $C_{24}H_{12}$, computed at the BP86/SVP level.

for the coronene molecule. Two basis sets, namely, an SVP (split valence polarization) and a TZ2P (triple-ζ double polarization) basis,[64] were used throughout this study.[65] All chemical shifts are given in ppm relative to the commonly used TMS (tetramethylsilane) standard.[66] All calculations were performed on single-processor DEC workstation computers.

Discussion of Results

To assess the accuracy of the quantum chemical calculations, it is essential to analyze, for a smaller model system, the dependence of the ^{1}H NMR chemical shifts not only on the methods and basis sets used for the calculation (GIAO-HF or GIAO-MP2, etc.) but also to study the influence of the structure for which the chemical shifts are computed. Although X-ray single-crystal structures are available for both coronene and HBC, it is more consistent to use computed geometries, since they are (1) fully reproducible, unlike, for example, X-ray structures, which always contain some experimental error margin, and (2) provide a consistent description of the electronic structure of a molecular system. In addition, in an X-ray structure, the C−H distances are generally not measured but instead simply added by some empirical approach. The use of an inappropriate C−H distance from the X-ray data can cause severe problems for the calculation of NMR chemical shifts as discussed elsewhere.[67]

For the study of methodological aspects, we consider first a single coronene molecule ($C_{24}H_{12}$; see Figure 2), which is expected to behave in a manner similar to that of the HBC systems and which is small enough to allow the study of methodological aspects. The study of coronene is followed by a discussion of the chemical shifts calculated for an isolated HBC monomer, where we estimate, in addition, the influence of substituents on the ^{1}H NMR chemical shifts. This forms the basis for the investigation of various fragments of possible solid-state arrangements, where dimer and trimer structures of HBC are chosen as model systems. In combination with the experimental ^{1}H NMR data, this finally allows the assignment of the solid-state structure for HBC-C_{12}.

Methodological Aspects. NMR data calculated at different levels of theory and structures for coronene and HBC are listed in Table 1, while calculated structural parameters are listed in Tables 2 and 3, respectively. Since the MP2 approach includes some of the electron correlation effects missing in the simple HF method, the value of 9.2 ppm obtained using the GIAO-MP2/SVP method at the MP2/SVP structure (notation: GIAO-MP2/SVP//MP2/SVP) for coronene is the most reliable one. The influence of the electron correlation effects included in the MP2 approach is −0.2 ppm comparing the value of 9.2 ppm with the one of 9.4 ppm at the GIAO-HF/SVP//MP2/SVP level. Basis set deficiencies in the GIAO-HF/SVP approach (as compared to GIAO-HF/TZ2P at the BP86/SVP structure) seem to lead to some fortuitous error compensation for the missing electron correlation effects, so that the GIAO-HF/SVP scheme seems to be a good compromise between reliability and computational costs for the study of the larger HBC systems.[68]

Using this GIAO-HF/SVP approach, it is possible to estimate the influence of structural parameters by comparing the results at the different geometries obtained at the HF, BP86, and MP2 level using an SVP basis: the calculated ^{1}H chemical shifts are

Table 1. Computed ^{1}H NMR Chemical Shifts for Coronene and HBC (Relative to TMS Standard)

molecule	method	structure	δ (^{1}H) [ppm]
coronene[a]	GIAO-HF/SVP	BP86/SVP	9.2
	GIAO-HF/SVP	HF/SVP	9.0
	GIAO-HF/SVP	MP2/SVP	9.4
	GIAO-HF/TZ2P	BP86/SVP	9.5
	GIAO-MP2/SVP	MP2/SVP	9.2
HBC	GIAO-HF/SVP	BP86/SVP	9.7/(8.4)[b]
	GIAO-HF/SVP	HF/SVP	9.6/(8.5)[b]

[a] The experimental ^{1}H NMR chemical shift was determined for a solution in $C_2D_2Cl_4$ to be 8.85 ppm and was found to be concentration independent. [b] The first value is for hydrogens H_1-H_{12} (D_{6h} symmetry) of HBC in Figure 3, whereas the value in parentheses corresponds to the six hydrogens (e.g., H_0) which are substituted in HBC-C_{12} by alkyl chains.

Table 2. Computed Structural Data for Coronene (D_{6h} Symmetry)

	BP86/SVP	HF/SVP	MP2/SVP
d(C1−C2) [pm]	143.4	140.1	142.5
d(C2−C3) [pm]	143.1	142.7	142.3
d(C3−C4) [pm]	138.4	135.7	137.9
d(C3−H3) [pm]	110.1	108.2	109.3
d(C1−C6) [pm]	143.4	142.9	142.6
∠(C1,C2,C3)	118.8°	118.9°	118.9°
∠(C2,C3,H3)	118.6°	118.8°	118.8°

Table 3. Computed Structural Data for Hexabenzocoronene (HBC, D_{6h} Symmetry)

	BP86/SVP	HF/SVP
d(C13−C14) [pm]	139.6	137.9
d(C14−C15) [pm]	141.2	139.4
d(C15−-C16) [pm]	146.5	146.9
d(C15−C17) [pm]	143.5	141.2
d(C17−C18) [pm]	145.1	145.7
d(C18−C19) [pm]	143.3	141.1
d(C13−H0) [pm]	110.0	108.2
d(C14−H12) [pm]	109.7	107.6
∠(C14,C15,C17)	119.2°	119.3°
∠(H12,C14,C15)	120.2°	120.8°
∠(C15,C17,C18)	120.4°	120.3°

(64) Schäfer, A.; Horn, H.; Ahlrichs, R. *J. Chem. Phys.* **1992**, *97*, 2571.

(65) The basis sets employ the following contraction patterns. SVP: (4s1p)/[2s1p] (for H) and (7s4p1d)/[3s2p1d] (for C). TZ2P: (5s2p1d)/[3s2p1d] (H) (10s6p2d1f)/[6s3p2d1f] (C). Spherical Gaussians were used in all calculations.

(66) The calculated ^{1}H absolute shieldings for TMS are 31.6 ppm (GIAO-HF/SVP//BP86/SVP), 32.1 ppm (GIAO-HF/SVP//HF/SVP), 31.9 ppm (GIAO-HF/SVP//MP2/SVP), 31.4 ppm (GIAO-HF/TZ2P//BP86/SVP), and 31.6 ppm (GIAO-MP2/SVP//MP2/SVP). The notation GIAO-HF/SVP//HF/SVP indicates here that the chemical shifts are computed at the GIAO-HF level using an SVP basis at the geometry obtained at the HF level employing an SVP basis.

(67) Ochsenfeld, C. *Phys. Chem. Chem. Phys.* **2000**, *2*, 2153.

(68) Basis set superposition errors (BSSE)[69] were investigated for a dimer structure of HBC, **Di_x3** (described later): replacing one monomer unit by dummy atoms holding the corresponding basis functions (SVP) changes the ^{1}H NMR chemical shifts by less than 0.1 ppm as compared to a simple HBC monomer structure, which indicates that no significant BSSE effects are expected in the calculation of chemical shifts)

(69) Boys, S. F.; Bernardi, F. *Mol. Phys.* **1970**, *19*, 553.

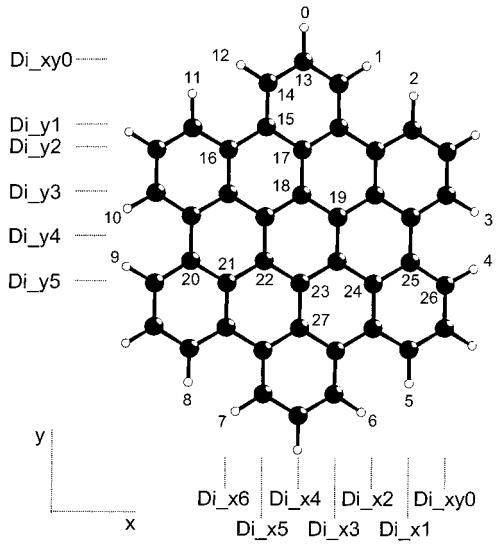

Figure 3. The structure of hexabenzocoronene, $C_{42}H_{18}$, computed at the BP86/SVP level. The hydrogen atom H_0 and its corresponding symmetry redundant atoms (D_{6h} symmetry) are substituted by alkyl chains in HBC-C_{12}. The markings at the bottom and on the left-hand side indicate the shift along the *x* and *y* axes, respectively, of the neighboring HBC molecule in the considered oligomer structures relative to the unshifted structure **Di_xy0**. The specified atom numbers serve to define the bond lengths and angles given in Table 3, the description of the considered dimers in Table 4, and the calculated ^{1}H NMR chemical shifts in Tables 5 and 6.

9.0, 9.2, and 9.4 ppm, respectively. These data can be considered as a good estimate for the maximum influence which can be caused by deficiencies in the description of structural parameters. Note that the bond alternation for the coronene structure is, as expected (see, e.g., ref 70 and references therein), larger at the HF than at the MP2 or BP86 level (see Table 2), indicating some deficiencies in the HF approach. The use of BP86/SVP structures is thus a reasonable compromise between accuracy and computational cost.

To assess the quality of describing the interactions between aromatic rings using the GIAO-HF/SVP approach, we studied a benzene dimer using both the GIAO-HF/SVP and GIAO-MP2/SVP method: the ^{1}H NMR shifts change by less than 0.2 ppm when correlation effects are included, which approves the use of the noncorrelated approach. Although a comparison with experimental data is not the aim of the calculations on coronene—rather we wish to determine the possible theoretical error margins—our most reliable gas-phase value of 9.2 ppm (GIAO-MP2/SVP//MP2/SVP) for coronene agrees well with the experimental solution-state value ($C_2D_2Cl_4$) of 8.85 ppm, even though no solvent effects have been considered. This study of methodological effects for the model system coronene leads us to the conclusion that the GIAO-HF/SVP//BP86/SVP approach is a reliable choice for the molecular systems to be investigated in the following.

HBC Monomer. An unsubstituted HBC monomer, showing D_{6h} symmetry, is depicted in Figure 3; the corresponding structural data are listed in Table 3. It should be noted that a structure with only D_6 symmetry (H atoms tilted slightly out of the carbon plane) was found to be energetically slightly less stable at the BP86/SVP level. For the relevant aromatic protons in HBC, the computed chemical shift is 9.7 ppm (GIAO-HF/SVP//BP86/SVP)—see Table 1. Performing the calculation at the HF/SVP rather than the BP86/SVP structure resulted in only a 0.1 ppm change in the calculated chemical shift—a similarly small change (0.2 ppm) was noted above for coronene.

(70) Choi, C. H.; Kertesz, M.; Karpfen, A. *J. Chem. Phys.* **1997**, *107*, 6712.

Table 4. Description of the Construction of Dimers/Trimers by Shifting One Monomer Unit Relative to a Second along Either the *x* or y Axis of HBC (see Figure 3)

structure	shifting axis	shifted distance[a]
Di_x1	*x*	$C_{25}-C_{24}$
Di_x2	*x*	$C_{25}-C_{19}$
Di_x3	*x*	$C_{25}-C_{23}$
Di_x4	*x*	$C_{25}-C_{22}$
Di_x5	*x*	$C_{25}-C_{21}$
Di_x6	*x*	$C_{25}-C_{20}$
Di_y1	*y*	$C_{14}-C_{16}$
Di_y2	*y*	$C_{13}-C_{17}$
Di_y3	*y*	$C_{13}-C_{18}$
Di_y4	*y*	$C_{17}-C_{27}$
Di_y5	*y*	$C_{13}-C_{23}$

[a] The shifted distance is defined as the difference between the coordinates of the two atoms (atom1−atom2) for the corresponding shifting axis.

The influence of alkyl substituents (HBC-C_{12}) can be estimated by calculating the chemical shifts in hexamethyl HBC (HBC-Me; hexamethylhexa-*peri*-hexabenzocoronene): the ^{1}H NMR shift changes only slightly from 9.7 to 9.5 ppm. Therefore, it is possible to neglect substituents for the study of dimer or trimer models which reduces the computational effort considerably.

A comparison of the computed value of 9.7 ppm for HBC (GIAO-HF/SVP//BP86/SVP) with experimental data is difficult since (1) unsubstituted HBC is only soluble under the most extreme conditions[49] and (2) the ^{1}H NMR shift recorded in solution for α-deuterated HBC-C_{12} depends strongly upon the HBC-C_{12} concentration: dilution changes the ^{1}H NMR shift to low field from 8.0 to 8.9 ppm.[32] This latter change can be understood as an indication of aggregation, i.e., the formation of oligomers, in solution, such that the "ring currents" of nearby molecules lead to shielding effects. Since the experimental value of 8.9 ppm for the HBC-C_{12} monomer does not correspond to infinite dilution, but rather to the point at which further dilution would be associated with prohibitively long measuring times, our computed value of 9.7 ppm for the HBC monomer is not unreasonable. Indeed, the ability to determine in this way the infinite-dilution chemical shift is very useful.

Construction of HBC Dimer and Trimer Model Systems. The simplest model for the investigation of molecular interactions in a solid-state column of HBC-C_{12} molecules is an HBC dimer structure. To construct such models, the position of one HBC monomer is fixed, while the position of the second is shifted systematically along either the *x* or *y* axis as illustrated in Figure 3. The exact shifting parameters for the considered arrangements are given in Table 4. To simplify the procedure, models corresponding to a simultaneous shift along both axes are not considered initially. The face-on and side-on views are shown in Figure 4 for two specific examples, namely, **Di_x3** and **Di_y3**. It should be noted that the **Di_x3** and the **Di_y2** structures correspond to the packing in the unsubstituted HBC system[49] and in graphite, respectively. In the latter case, half of the carbons are located directly above or below a carbon of the adjacent layer. This is to be compared to the former case, where none of the carbons are so aligned.

As a basis for the construction of dimer and also trimer models, the HBC monomer structure (BP86/SVP) was used, while an interplanar separation of 350 pm was chosen (for comparison, the interplanar distance found experimentally in

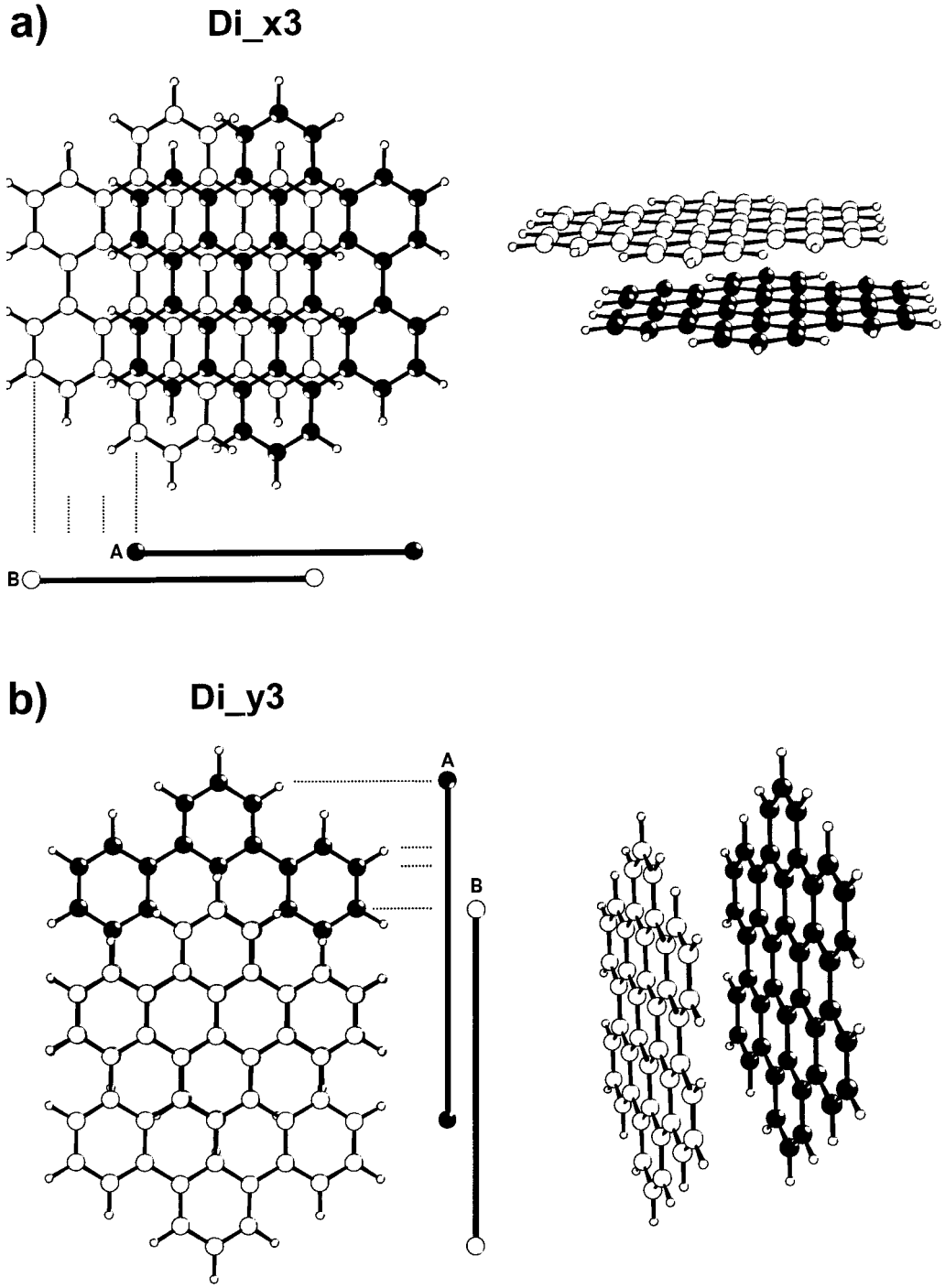

Figure 4. The arrangement of two HBC molecules in the (a) **Di_x3** and (b) **Di_y3** model structures. Face-on and side-on views are shown.

an X-ray study of unsubstituted HBC is 342 pm[49]). We will investigate the dependence of the NMR chemical shifts on the interplanar distance in a later part of this study.

The geometries of the dimers (and also of trimers) were not (re)optimized, since such structures would certainly be different from those within the solid state and thus—unlike the chosen model structures—not be faithful representations of the columns found in the solid state. Though neglection of geometrical relaxation effects is certainly an approximation, it is not expected to have dramatic effects on the conclusions drawn in this study (such a study is presented elsewhere in detail[67]).

It should be noted that the approach we adopt here assumes that the HBC cores are rigid on the time scale of the NMR experiment. Support for this assumption is provided by ^{1}H−^{1}H DQ MAS[32] and ^{1}H−^{13}C heteronuclear multiple-quantum[71] spinning-sideband patterns obtained for HBC-C_{12}, from which the dipolar couplings between the two bay aromatic protons and for the aromatic C−H pair were determined to be 15.0 ± 0.9 and 20.9 ± 0.5 kHz, respectively. The HBC cores can, thus, be assumed to be rigid, since, for the rigid case, these values correspond to the expected proton−proton and carbon−proton distances, respectively.

HBC Dimers. In Table 5 computed ^{1}H NMR shifts are listed for all the considered dimers. Hydrogen atoms H_7−H_9 correspond to atoms which are located further away from the neighboring HBC unit as compared to hydrogens H_1−H_3. The

(71) Fechtenkötter, A.; Saalwächter, K.; Harbison, M. A.; Müllen, K.; Spiess, H. W. *Angew. Chem., Int. Ed.* **1999**, *38*, 3039.

Table 5. Computed ^{1}H NMR Chemical Shifts (in ppm) for the HBC Model Dimers (see Figures 3 and 4; All C_{2h} Symmetry, with the Exception of the **Di_xy0** Structure Which Shows D_{6h} Symmetry)[a]

	H_1	H_2	H_3	H_7	H_8	H_9
Di_xy0[b]	9.3					
Di_x1[c]	8.7	8.7	8.3	9.3	9.4	9.6
Di_x2[c]	8.7	8.3	7.6	9.5	9.6	9.7
Di_x3[c]	8.9	7.9	6.9	9.7	9.8	9.8
Di_x4[c]	9.3	8.2	6.7	9.7	9.8	9.8
Di_x5[c]	9.5	8.7	6.4	9.8	9.8	9.8
Di_x6[c]	9.7	9.0	7.0	9.8	9.8	9.8
Di_y1[d]	7.9	7.9	9.0	9.7	9.7	9.2
Di_y2[d]	7.5	7.7	9.1	9.8	9.7	9.3
Di_y3[d]	7.2	8.0	9.2	9.9	9.9	9.7
Di_y4[d]	6.9	7.6	9.5	9.8	9.8	9.8
Di_y5[d]	7.0	8.0	9.8	9.8	9.8	9.8

[a] Experimental ^{1}H solid-state NMR data for HBC-C_{12}: 8.3, 6.9, and 5.7 ppm[32] (see Figure 1). [b] All hydrogens equivalent due to D_{6h} symmetry. [c] Second HBC shifted along the *x* axis (see Figure 3 and Table 4), such that $H_1 = H_6$, $H_2 = H_5$, $H_3 = H_4$, $H_7 = H_{12}$, $H_8 = H_{11}$, and $H_9 = H_{10}$. [d] Second HBC shifted along the *y* axis (see Figure 3 and Table 4), such that $H_1 = H_{12}$, $H_2 = H_{11}$, $H_3 = H_{10}$, $H_7 = H_6$, $H_8 = H_5$, and $H_9 = H_4$.

hydrogen shifts of atoms H_7-H_9 are therefore only given for completeness, since they are absent for an infinite columnar structure of HBC. For the unshifted stacked dimer, **Di_xy0**, it is a priori clear that there is only one aromatic ^{1}H NMR signal (two without substituents, of course) due to its D_{6h} symmetry. However, it is interesting to observe that the influence of molecular interactions gives a 0.4 ppm shift relative to the isolated molecule. As noted above, three aromatic resonances at 8.3, 6.9, and 5.7 ppm are observed in the experimental solid-state spectra of HBC-C_{12}. An inspection of the calculated chemical shifts for atoms H_1, H_2, and H_3 listed in Table 5 reveals that not all of the model dimers yield a similar pattern consisting of equally spaced peaks. Of those that do, the discrepancies as compared with the experimental values are quite large: 0.6−1.2 ppm for **Di_x3**, 0.7−1.2 ppm for **Di_y4**, 1.0−1.3 ppm for **Di_x4**, 0.9−1.5 ppm for **Di_y3**, and 0.4−1.9 ppm for **Di_x2**. Even the dimer structure **Di_y5** with deviations of 1.1−1.5 ppm shows a crudely similar pattern. However, this structure can be discarded due to its extremely strong deviation from a vertical column, such that it would presumably lead to a particularly unfavorable structure. This has reduced the number of possibilities from 12 to 6 structures.

The large deviations between the experimental and calculated shifts for all the remaining structures must now be addressed. In Figure 5, the dependence of ^{1}H NMR shifts on the interplanar distance is displayed using **Di_x3** as an example. It can be seen that even at 700 pm, which corresponds to twice the original distance, the interaction of the aromatic rings influences the ^{1}H NMR chemical shifts: the pattern changes from 8.9, 7.9, 6.9 ppm at 350 pm to 9.2, 9.0, 8.6 at 700 pm. The chemical shifts in the latter case are still significantly different from the value of 9.7 ppm for an isolated HBC monomer. Moreover, even at three times the original distance, a convergence to the isolated HBC monomer value has still not been reached. Therefore, the simple dimer model needs to be extended to include at least one further layer, as will be described in the next section. It should be noted that decreasing the interplanar distance from 350 to 340 pm has only a negligible influence on the calculated ^{1}H NMR shifts (less than 0.1 ppm).

HBC Trimers. The trimers are constructed in the same way as the corresponding dimers by the addition of one further layer (see, for example, Figure 6). The computed ^{1}H NMR chemical shifts are listed in Table 6. For the trimer structures, two layers can be distinguished: the edge layer which has two neighbors on one side and the middle layer which has neighbors on both sides. For the middle layers, all of the ^{1}H NMR chemical shifts are meaningful in modeling an infinite stacked column. This is to be compared to the edge layer (and to the dimer) where only the shifts of H_1-H_3 are of interest, since the computed values for H_7-H_9 are of no relevance for an infinite column.

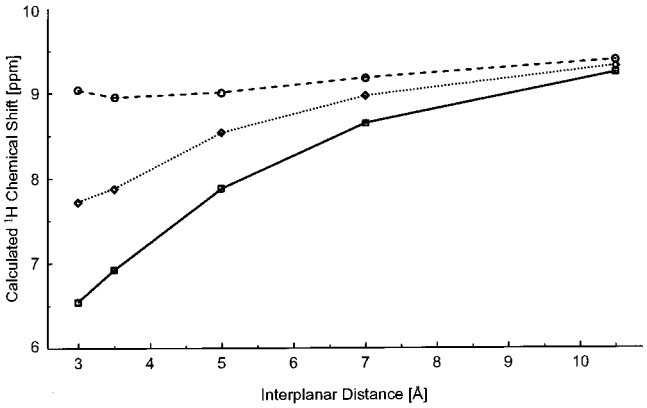

Figure 5. The dependence of the calculated ^{1}H NMR shifts at the GIAO-HF/SVP level on the interplanar distance for the **Di_x3** model structure (lines linking the calculated points serve as a guide to the eye).

Comparing Tables 5 and 6, it can be seen that the ^{1}H NMR shifts for the trimer middle layer change by no more than 0.1−0.3 ppm in comparison to the relevant corresponding values for the dimers. This leads to the conclusion that the influence of "sandwiching" an HBC monomer has only minor effects.

In contrast, an inspection of the values for the edge layer reveals significant changes in the ^{1}H NMR shifts as compared to the dimer structure, a fact which is to be expected on the basis of the study of the interplanar distance dependence (Figure 5) discussed earlier. If the values for the trimer edge layer are compared to the experimentally observed ^{1}H NMR shifts of 8.3, 6.9, and 5.7 ppm, the agreement is significantly improved compared to the case of the dimer models used above. The best agreement is found for **Tri_x3** with a deviation of 0.2−0.5 ppm. Deviations for other dimer models are larger: 0.0−0.8 ppm for **Tri_x2**, 0.5−0.8 ppm for **Tri_y3**, 0.3−1.1 ppm for **Tri_x4**, and 0.5−1.3 ppm for **Tri_y4**. These differences will be further reduced by roughly 0.2 ppm if alkyl-substituent effects are taken into account, assuming the same trend for the trimers as for the monomer. Similarly small changes in the calculated chemical shifts could also be expected due to the sandwiching effects described above.

In Figure 5, the calculated ^{1}H chemical shifts for a separation of 1050 ppm deviate by between 0.3 and 0.5 ppm from the value for an isolated HBC molecule. The question then arises, is it necessary to consider a tetramer model? It must, however, be noted that the calculated values in Figure 5 correspond to the location of two HBC cores in the **Di_x3** arrangement. In an x3 tetramer, the relative displacement of the two edge HBC cores is three times greater, such that, when viewed in the face-on fashion, the two edge HBC cores have no direct overlap, and thus their interaction is expected to influence the chemical shifts by less than the 0.3−0.5 ppm observed in Figure 5. In addition, it is possible to estimate by a comparison of dimer and trimer values the chemical shifts for the middle layer in a pentamer (similar to the discussion in ref 67): the changes as compared to the edge layer of the trimer **Tri_x3** are found to be 0.2 ppm at most. Therefore, these effects are of less

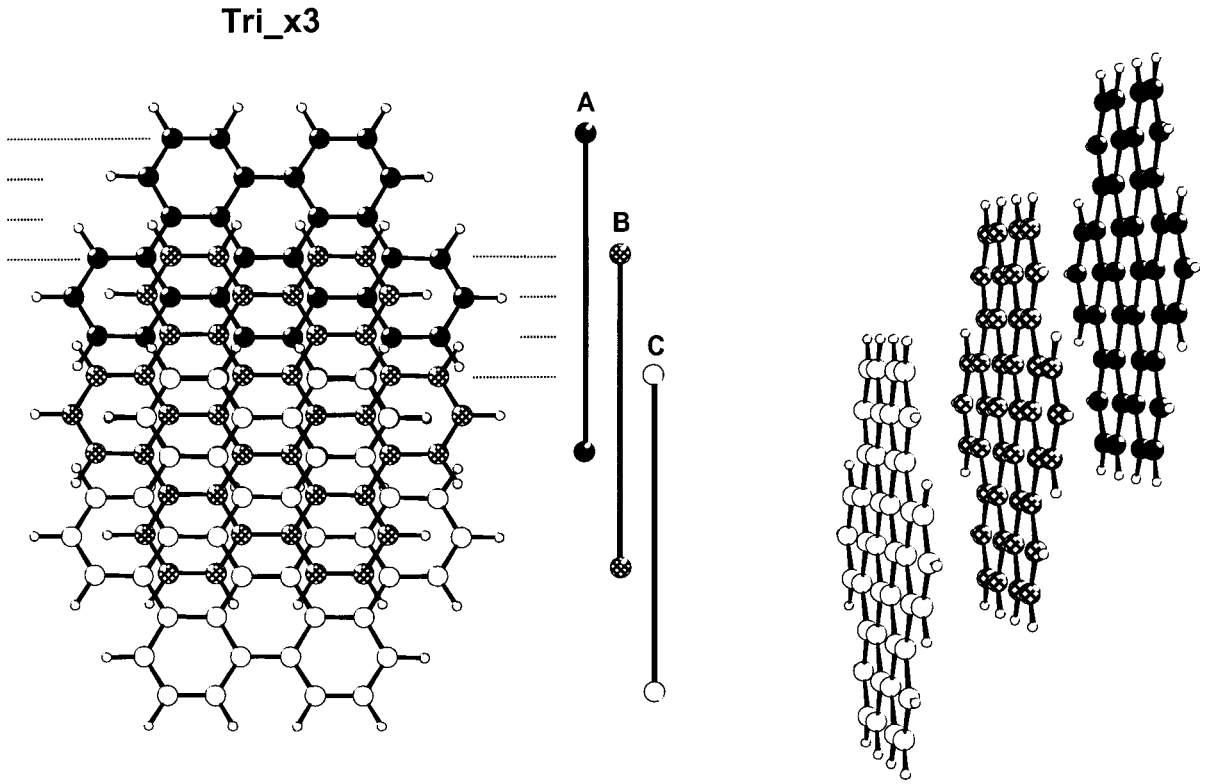

Figure 6. The **Tri_x3** model structure. Face-on and side-on views are shown.

Table 6. Computed NMR Chemical Shifts (in ppm) for the HBC Model Trimers (C_{2h} Symmetry). Data for the Edge and Middle HBC Layers Are Listed[a]

molecule	layer	H_1	H_2	H_3	H_7	H_8	H_9
Tri_x2[b]	edge	8.3	7.7	6.5	9.3	9.5	9.7
	middle[d]	8.4	8.2	7.6			
Tri_x3[b]	edge	8.7	7.4	5.9	9.6	9.8	9.8
	middle[d]	9.0	8.0	7.1			
Tri_x4[b]	edge	9.2	8.0	6.0	9.8	9.8	9.8
	middle[d]	9.4	8.3	6.8			
Tri_x5[b]	edge	9.5	8.6	6.1	9.8	9.8	9.8
	middle[d]	9.6	8.8	6.5			
Tri_y3[c]	edge	6.2	7.4	9.1	9.9	9.9	9.7
	middle[d]	7.3	8.2	9.3			
Tri_y4[c]	edge	6.5	7.4	9.6	9.8	9.8	9.9
	middle[d]	7.0	7.8	9.7			

[a] Experimental ^{1}H NMR data for the solid-state structure of HBC-C_{12}: 8.3, 6.9, and 5.7 ppm[32] (see Figure 1). [b] Trimer where the HBC molecules are shifted along the *x* axis (see Figure 6), such that $H_1 = H_6$, $H_2 = H_5$, $H_3 = H_4$, $H_7 = H_{12}$, $H_8 = H_{11}$, and $H_9 = H_{10}$. [c] Trimer where the HBC molecules are shifted along the *y* axis (see Figure 6), such that $H_1 = H_{12}$, $H_2 = H_{11}$, $H_3 = H_{10}$, $H_7 = H_6$, $H_8 = H_5$, and $H_9 = H_4$. [d] Since the middle HBC is neighbored by HBC molecules on each side (C_{2h} symmetry), the following further hydrogens are equivalent: $H_1 = H_7$, $H_2 = H_8$, and $H_3 = H_9$.

importance than the influence of alkyl substituents or sandwiching, and it is thus not necessary to further increase the size of the considered model structures.

The results given above lead to the conclusion that the experimental MAS NMR spectrum[32] can be most likely explained by the **Tri_x3** structure. However, within the experimental and theoretical error bars, the spectrum could also fit to the **Tri_y3** or the **Tri_x2** structure, though in both cases the agreement between theory and experiment is poorer. In contrast, it appears that the other structures can be discarded.

Distinction of Packing Arrangements by ^{1}H−^{1}H Proximities. So far only the calculated chemical shifts themselves have been considered. This leaves an ambiguity, because the calculated ^{1}H chemical shifts are similar for the **Tri_x2**, **Tri_x3**, and **Tri_y3** model structures. Further discrimination is possible if the ^{1}H DQ NMR spectra are considered: in addition to the chemical shifts of the different ^{1}H sites, the presence of particular DQ peaks reflect the ^{1}H−^{1}H proximities. As demonstrated in Figures 7a and 7b, the DQ patterns for structures **Tri_x3** and **Tri_y3** are very different in that the most and least shielded protons, respectively, form an auto pair (diagonal peak). Note that the expected pattern for **Tri_x2** is of the same form as that for **Tri_x3**. Clearly only the pattern in Figure 7a is in agreement with the experimental spectrum in Figure 7c. Thus, only the **Tri_x2** and the **Tri_x3** model systems remain in consideration. In this respect, it should be stressed that the **Tri_x2** is geometrically fairly close to the **Tri_x3** structure and that it can be expected that smaller shifts of the monomer layers (along the *x* axis) around the chosen structures will not change the ^{1}H NMR spectrum abruptly.

It should be noted that only model structures involving a shift along either the *x* or *y* axes have been considered so far. To investigate the effect of a simultaneous shift along both the *x* and *y* axes, a dimer was constructed, in which, starting from the **Di_x3** arrangement, the second HBC core was additionally shifted by 50 pm along the *x* (toward the **Di_x2** arrangement) and *y* (from the **Di_xy0** toward the **Di_y1** arrangement) axes. In this way, the *x* shift corresponds to a position almost midway between the **Di_x2** and **Di_x3** arrangements. The relevant calculated ^{1}H chemical shifts for this dimer are $H_1 = 9.0$ ppm, $H_2 = 8.3$ ppm, $H_3 = 7.2$ ppm, $H_4 = 7.1$ ppm, $H_5 = 7.7$ ppm, and $H_6 = 8.5$ ppm. Unlike the case for a shift along only one axis, it is clear that a simultaneous shift along both axes leads to six rather than three aromatic protons possessing different ^{1}H chemical shifts. Note that, for this shift of 50 pm, which corresponds to approximately only a third of a C−C bond length, the previously equivalent H_1 & H_6 and H_2 & H_5 chemical shifts differ by at least 0.5 ppm. In this way, structures involving a simultaneous shift along both axes can be excluded, although

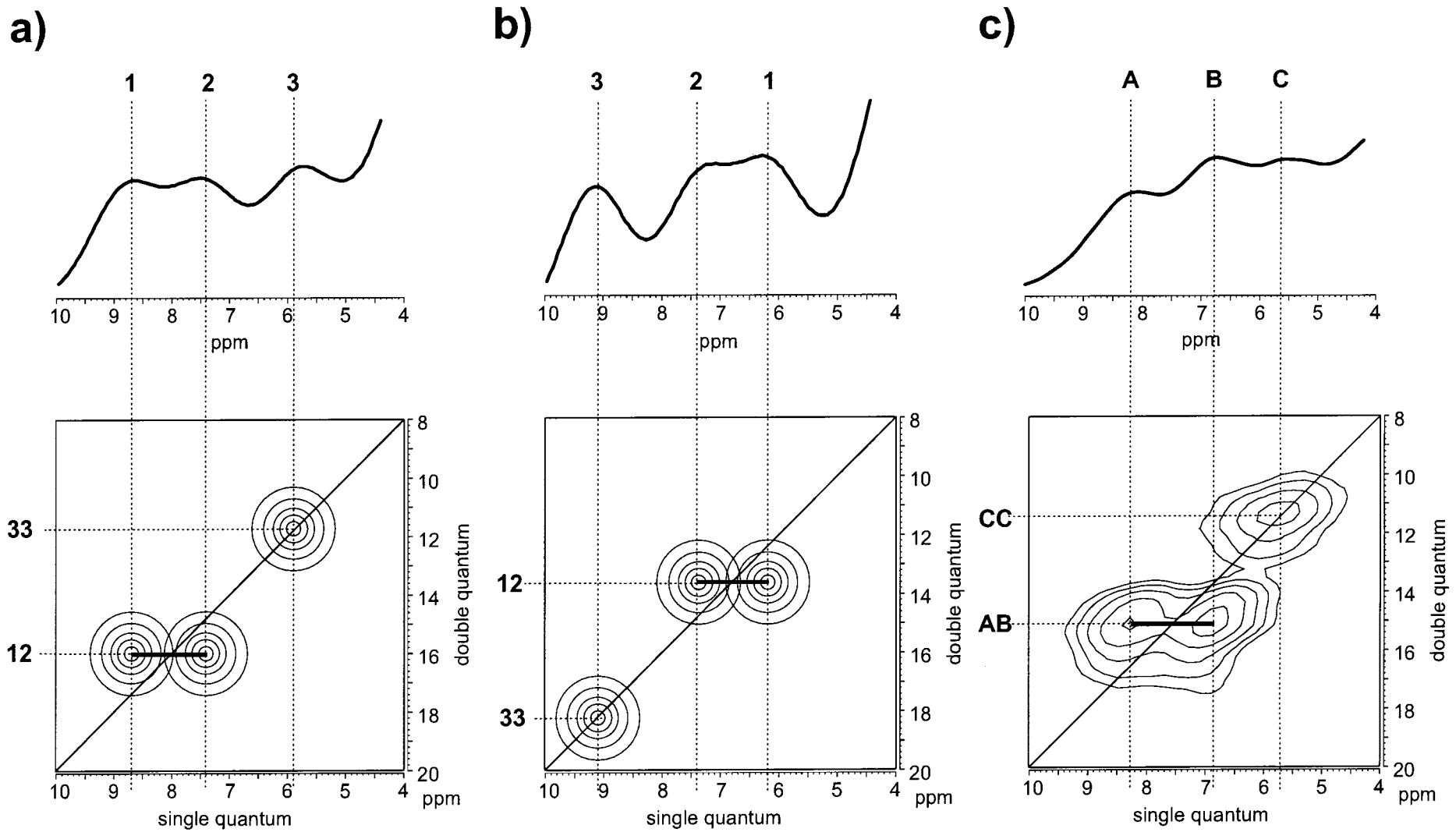

Figure 7. Calculated 1D spectra and schematic 2D DQ spectra corresponding to the calculated ^{1}H NMR chemical shifts given in Table 6 for the (a) **Tri_x3** and (b) **Tri_y3** model structures. For **Tri_y3**, by symmetry arguments, it is apparent that $H_3 = H_4$ for an infinite column. In the calculated one-dimensional spectra, all aromatic resonances are represented by Gaussian line shapes having the same half-width at half-maximum height of 0.8 ppm—in addition, to mimic the experimental spectrum, the contribution of the shoulder of the intense alkyl peak is also included. To allow a direct comparison, the experimental spectra shown in Figure 1, are repeated in (c).

it should be noted that, given the experimental ^{1}H line width of about 1.5 ppm, such a structure would be expected to give rise to less rather than more resolved aromatic resonances in the experimental spectrum. To appreciate this latter point, consider the effect of summing six Gaussian lines with the experimental line width at the above chemical shifts: the net effect will be a broad hump, where at best a single shoulder will be resolved. Moreover, the difference between the two cases would be particularly apparent in the two-dimensional ^{1}H DQ MAS spectra.

Returning to the discussion of Table 6, since the difference between the experimental and calculated chemical shifts is more pronounced for the **Tri_x2** structure, we conclude that, within the accuracy of our approach, the **Tri_x3** structure describes the actual packing of the HBC cores in the solid-state structure of HBC-C_{12}.

Conclusion

In this paper, we have shown how quantum chemical calculations allow experimental ^{1}H solid-state NMR spectra to be assigned in a quantitative manner to a specific molecular packing. This approach is based on the marked sensitivity of the ^{1}H chemical shift to ring currents arising from nearby (in space) aromatic rings. In particular, the calculations revealed that these ring current effects are long-range interactions, with a considerable influence of the second neighbor (at a distance of 700 pm) being observed. Moreover, the value of the proximity information inherent to ^{1}H DQ MAS NMR spectroscopy has again been illustrated.

This study has identified the packing of the HBC cores in the solid-state phase of HBC-C_{12} to be of the **Tri_x3** type; this corresponds to the arrangement of HBC molecules in the X-ray single-crystal structure of unsubstituted HBC and confirms the hypothesis presented in ref 32. It should be noted that changing some or all of the alkyl substituents can lead to significantly different packing arrangements. For example, we have recently shown that the ^{1}H DQ MAS spectrum recorded for HBC-*t*Bu, where the six alkyl substituents are *tert*-butyl groups, is quite different than that observed for HBC-C_{12}.[33] In this case, an X-ray single-crystal structure is available, which shows that the bulky substituents force the HBC cores to adopt a different structure, consisting of pairs of molecules in a sandwich-like arrangement. In a parallel investigation to this one, quantum chemical shift calculations have assigned the experimental ^{1}H NMR spectra.[67] In this way, the combined experimental and theoretical approach should be able to provide much useful information about not only other alkyl-substituted HBC derivatives but also other unknown structures.

Moreover, we emphasize that, for the NMR experiments, there is no requirement for isotopic labeling or the preparation of single crystals, with only 10 mg of sample being needed, while the measuring times are short because of the excellent sensitivity of ^{1}H NMR. Furthermore, as noted in the Introduction, heteronuclear ^{1}H−^{13}C correlation experiments applicable to naturally abundant samples have recently been developed.[42−44] These experiments provide information which is complementary to the information about proton−proton proximities provided by ^{1}H homonuclear DQ MAS NMR. As an example, the ^{1}H−^{13}C correlation spectrum of L-tyrosine reveals that distinct ^{1}H resonances are observed for the chemically equivalent (for an isolated molecule) aromatic protons; this phenomenon is again attributable to intermolecular ring current effects. As stated in the Introduction, heteronuclear experiments employing homonuclear ^{1}H decoupling methods yield, for model compounds, significantly narrower ^{1}H line widths than those observed in the ^{1}H MAS and DQ MAS spectra presented in Figure 1; the ongoing development of these methods offers the promise of routinely allowing a much better resolution of the ^{1}H peaks in systems like HBC-C_{12}.

To conclude, we believe that the combined use of solid-state NMR spectroscopy and quantum chemical NMR chemical shift calculations will develop into a powerful tool for future investigations of molecular arrangements in condensed phases, in particular for disordered systems where no X-ray single-crystal structure is available, e.g., liquid crystals and amorphous materials. This approach is also expected to be of much value in supramolecular chemistry applications,[72] where intermolecular nonbonding interactions are of much importance, e.g., we have further applied these methods to molecular tweezer host−guest systems[35] and are also currently working on extending the approach to hydrogen-bonded systems. Finally, the ongoing methodological advances in both solid-state NMR spectroscopy and the quantum chemical treatment of large molecular systems will further enhance this fruitful interplay of experiment and theory.

Acknowledgment. We thank Prof. Dr. Reinhart Ahlrichs (Universität Karlsruhe) for the possibility to use the program package TURBOMOLE. In addition, the authors thank Andreas Fechtenkötter and Dr. Kay Saalwächter (MPIP Mainz) for informative discussions and Dr. Manfred Wagner and Dr. Florian Dötz (MPIP Mainz) for carrying out the solution-state NMR investigation of coronene. C.O. acknowledges financial support by a Liebig "Habilitation" fellowship from the Fonds der Chemischen Industrie. S.P.B. thanks the Alexander von Humboldt-Stiftung for the award of a research fellowship.

JA0021823

(72) *Comprehensive Supramolecular Chemistry*; Atwood, J. L., Davies, J. E. D., MacNicol, D. D., Vögtle, F.; Lehn, J.-M., Eds.; Elsevier: Oxford, 1996.